Side Chain-modified Benzothiazinone Derivatives with Anti-Mycobacterial Activity

Dongguang Fan[1], Bin Wang[2], Giovanni Stelitano[3], Karin Savková[4], Olga Riabova[5], Rui Shi[1], Xiaomei Wu[1], Laurent R. Chiarelli[3], Katarína Mikušová[4], Vadim Makarov[5], Yu Lu[2], Yuzhi Hong[6,7] and Chunhua Qiao [1,7]*

[1] College of Pharmaceutical Sciences, Suzhou Medical College, Soochow University, 199 Renai Road, Suzhou, P.R. China.

[2] Beijing Key Laboratory of Drug Resistance Tuberculosis Research, Department of Pharmacology, Beijing Tuberculosis and Thoracic Tumor Research, Beijing Chest Hospital, 97 Ma Chang Street, Beijing, 101149, P.R. China.

[3] Department of Biology and Biotechnology, University of Pavia, 27100 Pavia, Italy

[4] Department of Biochemistry, Faculty of Natural Sciences, Comenius University in Bratislava, 842 15 Bratislava, Slovakia.

[5] Research Center of Biotechnology of the Russian Academy of Sciences, Moscow 119071, Russia.

[6] Institute of Molecular Enzymology & School of Biology and Basic Medical Sciences, Suzhou Medical College, Soochow University, P.R. China

[7]. Suzhou Key Laboratory of Pathogen Bioscience and Anti-infective Medicine, Suzhou Medical College, Soochow University, 199 Renai Road, Suzhou, P.R. China.

* Correspondence: qiaochunhua@suda.edu.cn

Abstract: Tuberculosis (TB) is a leading infectious disease with serious antibiotic resistance. The benzothiazinone (BTZ) scaffold PBTZ169 kills *Mycobacterium tuberculosis* (Mtb) through the inhibition of the essential cell wall enzyme decaprenylphosphoryl-β-D-ribose 2'-oxidase (DprE1), PBTZ169 shows anti-TB potential in animal model and piloted clinical tests. Although highly potent, the BTZ type DprE1 inhibitors in general shows extremely low aqueous solubility, which adversely affects the drug like properties. To improve the compounds physiochemical properties, we generated a series of BTZ analogues. Several optimized compounds had MIC values against Mtb in single digit nanomolar. The representative compound **37** displayed improved solubility and bioavailability compared to the lead compound. Additionally, compound **37** shows Mtb-killing ability in an acute infection mouse model.

Keywords: Anti-tubercular agents; DprE1 inhibitor; Structure activity relationship; *in vivo* activity

1. Introduction

The notorious infectious disease tuberculosis (TB) is listed as one of the top death-leading infectious diseases worldwide. The reported mortality is 1.4 million each year, and an estimated latent infection of 2 billion people[1]. Treatment of the disease using the first-line anti-tubercular agents: isoniazid, rifampicin, ethambutol, pyrazinamide and streptomycin, is challenged as more and more reported cases of multidrug resistant (MDR) and extensively drug-resistant (XDR) clinical mutants[2]. To combat with the disaster of MDR- and XDR-TB, conscious and concerted efforts continued to discover anti-TB antibiotics with new targets or scaffolds over the past decades.

A class of compounds with a benzothiazinone (BTZ) scaffold, first reported in 2009, show potent antitubercular activity, and inhibit the essential cell wall biosynthesis enzyme decaprenylphosphoryl-*β*-D-ribose 2′ oxidase (DprE1)[3,4,5]. Among all reported BTZ derivatives, BTZ043 and PBTZ169[6] (**Figure 1**) attracted most attention because of their remarkable whole-cell activity, with the minimal inhibitory concentration (MIC) values lower than 1.0 ng/mL. On top of this, the BTZ type candidates demonstrated synergistic effect with other TB drugs[6]. Reported

studies have shown that the BTZ type DprE1 inhibitors are active against MDR and XDR strains[3]. Although both benzothiazinones have been advanced to clinical trials, each suffered suboptimal drug like properties. In addition to their low aqueous solubility, the presence of a chiral center in BTZ043 renders its synthesis disadvantageous; the more potent second generation PBTZ169 takes liability of poor *in vivo* bioavailability, presumably emanating from its low water solubility and high plasma protein binding fraction [7].
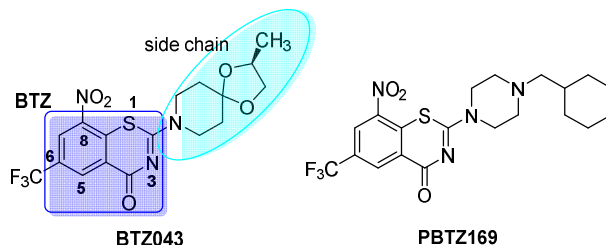
Figure 1. Structures of BTZ043 and PBTZ169.

To improve the BTZ type compounds physiochemical properties, we herein report our investigation of novel series of derivatives with improved aqueous solibility and good pharmacokinetic activity. We demonstrated side chain modification by opening the cyclic piperidinyl or piperzinyl ring could expand the BTZ compound diversity, and afford BTZ analogs with elevated physicochemical properties.

2. Materials and Methods

2.1. General Experimental Information

Reagents, solvents and materials were purchased from commercial suppliers and were used directly, unless further treatment was noted. Anhydrous solvent tetrahydrofuran (THF) and dichloromethane (DCM) were also obtained and used as commercial sources. Thin layer chromatography (TLC) were monitored and performed on silica HSGF254 plates to follow the reations. TLC was virulized by ultraviolet light (UV) light at 254 or 365 nm, or exposure to I_2. The crude product purification were conducted on column chromatography silica gel (300–400 mesh). All final products were recorded ^{1}H NMR,^{13}C NMR on an Agilent–400 MHz or Bruker DD2-600 MHz spectrometer in CDCl$_3$ or dimethyl sulfoxide (DMSO-d$_6$), TMS was used as reference. High resolution mass analysis (HRMS) in electrospray ionization mode was determined on Micromass GCT-TOF. The sample purity analysis was determined by high performance liquid chromatography (HPLC) on SHIMADZU LC–20AD system. Before sending for biological test, all tested compounds purity is greater than 95%.

Abbreviations: PEG: poly ethylene glycol; HCl: hydrochloric acid; DMF: *N,N*-dimethylformamide; DCM: dichloromethane; MeOH: methanol; CDI: 1,1'-carbonyldiimidazole; ESI: electrospray ionization.

2.2. Characterization Data for the Compounds

BTZ: 8-nitro-6-(trifluoromethyl)-4H-benzo[e][1,3]thiazin-4-one

2-(((1-cyclohexyl-1H-1,2,3-triazol-4-yl)methyl)(methyl)amino)-BTZ (1). yield 53%; Solid, yellow color; ^{13}C NMR (151 MHz, CDCl$_3$) δ: 163.3, 166.1, 141.4, 143.9, 133.7 (d, J = 2.2 Hz), 134.4, 130.0 (q, J = 35.6 Hz), 126.0 (d, J = 2.6 Hz), 126.7, 122.5 (q, J = 273.3 Hz), 121.6, 46.7, 60.5, 37.0, 25.3, 33.6, 25.2; ^{1}H NMR (400 MHz, CDCl$_3$) δ: 9.13 (s, 1H), 8.77 (s, 1H), 7.77 (s, 1H), 5.12 (s, 2H), 4.43 – 4.37 (m, 1H), 3.51 (s, 3H), 2.16 (d, J = 8.0 Hz, 2H), 1.90 (d, J = 8.0 Hz, 2H), 1.76 – 1.70 (m, 2H), 1.47 – 1.38 (m, 2H), 1.30 – 1.25 (m, 2H); HRMS-ESI *(m/z)* calcd [M+H]$^+$ for C$_{19}$H$_{20}$F$_3$N$_6$O$_3$S$^+$ 469.1264, found 469.1259.

2-(methyl((1-phenyl-1H-1,2,3-triazol-4-yl)methyl)amino)-BTZ (2). yield 43%; Solid, white; ^{13}C NMR (151 MHz, CDCl$_3$) δ: 166.1, 163.4, 144.1, 142.5, 136.8, 134.2, 133.6 (d, J = 3.0 Hz), 130.0 (q, J = 36.1 Hz), 123.0, 129.0, 126.7, 126.1 (d, J = 3.0 Hz), 122.4 (q, J = 273.2 Hz), 122.3, 120.6, 46.7, 37.0; ^{1}H NMR

(400 MHz, CDCl$_3$) δ: 9.13 (s, 1H), 8.76 (s, 1H), 8.24 (s, 1H), 7.70 (d, *J* = 7.60 Hz, 2H), 7.51 (t, *J* = 7.2 Hz, 2H), 7.44 (d, *J* = 7.2 Hz, 1H), 5.20 (s, 2H), 3.57 (s, 3H); HRMS-ESI *(m/z)* calcd [M+H]$^+$ for C$_{19}$H$_{14}$F$_3$N$_6$O$_3$S$^+$ 463.0795, found 463.0797.

2-(ethyl((1-phenyl-1H-1,2,3-triazol-4-yl)methyl)amino)-BTZ (3). yield 43%; Solid, white; ^{13}C NMR (151 MHz, CDCl$_3$) δ: 166.2, 162.6, 144.1, 142.9, 137.0, 134.5, 133.6, 129.9, 129.9 (q, *J* = 34.7 Hz), 129.1, 126.8, 126.2 (d, *J* = 3.0 Hz), 122.9, 122.5 (q, *J* = 273.3 Hz), 120.7, 45.1, 44.7, 13.1; ^{1}H NMR (400 MHz, CDCl$_3$) δ: 9.12 (s, 1H), 8.76 (s, 1H), 8.33 (s, 1H), 7.71 (d, *J* = 8.0 Hz, 2H), 7.50 (t, *J* = 7.4 Hz, 2H), 7.43 (d, *J* = 6.8 Hz, 1H), 5.13 (s, 2H), 3.98 (q, *J* = 7.0 Hz, 2H), 1.50 (t, *J* = 3.8 Hz, 3H); HRMS-ESI *(m/z)* calcd [M+H]$^+$ for C$_{20}$H$_{16}$F$_3$N$_6$O$_3$S$^+$ 477.0951, found 477.0944.

2-(((1-benzyl-1H-1,2,3-triazol-4-yl)methyl)(methyl)amino)-BTZ (4). yield 40%; A white solid; ^{13}C NMR (151 MHz, CDCl$_3$) δ: 166.1, 163.4, 144.0, 142.3, 134.4, 134.4, 133.6 (d, *J* = 36.1 Hz), 130.0 (q, *J* = 36.1 Hz), 129.3, 129.0, 128.3, 126.7, 126.1 (d, *J* = 3.0 Hz), 123.9, 122.5 (q, *J* = 273.3 Hz), 54.3, 46.3, 36.8; ^{1}H NMR (400 MHz, CDCl$_3$) δ: 9.12 (s, 1H), 8.78 (s, 1H), 7.72 (s, 1H), 7.36 (br, 3H), 7.28 (br, 2H), 5.50 (s, 2H), 5.11 (s, 2H), 3.51 (s, 3H); HRMS-ESI *(m/z)* calcd [M+H]$^+$ for C$_{20}$H$_{16}$F$_3$N$_6$O$_3$S$^+$ 477.0951, found 477.0944.

2-(methyl((1-(pyridin-4-yl)-1H-1,2,3-triazol-4-yl)methyl)amino)-BTZ (5). yield 49%; A yellow solid; ^{13}C NMR (151 MHz, CDCl$_3$) δ: 166.1, 163.6, 151.7, 144.0, 143.4, 142.6, 134.3, 133.7 (d, *J* = 2.9 Hz), 130.1 (q, *J* = 35.9 Hz), 126.7 (d, *J* = 3.3 Hz), 126.3 (d, *J* = 3.3 Hz), 122.5 (q, *J* = 273.2 Hz), 121.9, 46.8, 37.2; ^{1}H NMR (400 MHz, DMSO-d_6) δ: 9.00 (s, 1H), 8.88 (s, 2H), 8.82 (br, 2H), 7.98 (s, 2H), 5.21 (s, 2H), 3.44 (s, 3H); HRMS-ESI *(m/z)* calcd [M+H]$^+$ for C$_{18}$H$_{13}$F$_3$N$_7$O$_3$S$^+$ calculated 464.0747, found 464.0748.

2-(methyl((1-(pyridin-3-yl)-1H-1,2,3-triazol-4-yl)methyl)amino)-BTZ (6). yield 57%; A yellow solid; ^{13}C NMR (151 MHz, CDCl$_3$) δ: 166.2, 163.6, 150.3, 150.2, 144.0, 143.2, 141.9, 134.3, 133.5 (d, *J* = 2.6 Hz), 130.1 (q, *J* = 35.5 Hz), 128.1, 126.6, 126.2 (d, *J* = 2.9 Hz), 122.5, 122.5 (q, *J* = 273.3 Hz), 121.6, 46.7, 37.3; ^{1}H NMR (400 MHz, CDCl$_3$) δ: 9.12 (s, 1H), 9.04 (s, 1H), 8.77 (s, 1H), 8.72 (brs, 1H), 8.35 (brs, 1H), 8.08 (d, *J* = 7.4 Hz, 1H), 7.50 (brs, 1H), 5.20 (s, 2H), 3.58 (s, 3H); HRMS-ESI *(m/z)* calcd [M+Na]$^+$ for C$_{18}$H$_{12}$F$_3$N$_7$NaO$_3$S$^+$ 486.0567, found 486.0547.

2-(((1-([1,1'-biphenyl]-4-yl)-1H-1,2,3-triazol-4-yl)methyl)(methyl)amino)-BTZ (7). yield 64%; A yellow solid; ^{13}C NMR (151 MHz, CDCl$_3$) δ: 166.2, 163.5, 144.0, 142.6, 142.1, 139.6, 136.0, 134.4, 133.7, 130.0 (q, *J* = 35.49 Hz), 129.1, 128.5, 128.2, 127.2, 126.7, 126.2 (d, *J* = 2.6 Hz), 122.6 (q, *J* = 273.1 Hz), 122.2, 120.9, 46.8, 37.0; ^{1}H NMR (400 MHz, CDCl$_3$) δ: 9.14 (s, 1H), 8.77 (s, 1H), 8.30 (s, 1H), 7.79 (d, *J* = 8.0 Hz, 2H), 7.72 (d, *J* = 8.0 Hz, 2H), 7.60 (d, *J* = 7.2 Hz, 2H), 7.47 (t, *J* = 7.4 Hz, 2H), 7.39 (t, *J* = 7.2 Hz, 1H), 5.21 (s, 2H), 3.59 (s, 3H); HRMS-ESI *(m/z)* calcd [M+H]$^+$ for C$_{25}$H$_{18}$F$_3$N$_6$O$_3$S$^+$ 539.1108, found 539.1108.

2-(methyl((1-(naphthalen-2-yl)-1H-1,2,3-triazol-4-yl)methyl)amino)-BTZ (8). yield 67%; yellow solid; ^{13}C NMR (151 MHz, CDCl$_3$) δ: 166.2 163.6, 134.4, 134.3, 133.6 (d, *J* = 3.4 Hz), 133.3, 133.1, 130.2, 129.9 (q, *J* = 35.48 Hz), 128.4, 128.1, 127.7, 127.3, 126.6, 126.2 (d, *J* = 2.6 Hz), 122.5 (q, *J* = 273.1 Hz), 122.4, 118.9, 118.7, 46.7, 37.1; ^{1}H NMR (400 MHz, CDCl$_3$) δ: 9.14 (d, *J* = 1.6 Hz, 1H), 8.77 (d, *J* = 1.6 Hz, 1H), 8.39 (s, 1H), 8.16 (d, *J* = 1.6 Hz, 1H), 7.99 (d, *J* = 8.8 Hz, 1H), 7.93 – 7.86 (m, 3H), 7.60 – 7.54 (m, 2H), 5.24 (s, 2H), 3.60 (s, 3H); HRMS-ESI *(m/z)* calcd [M+H]$^+$ for C$_{23}$H$_{16}$F$_3$N$_6$O$_3$S$^+$ 513.0951, found 513.0949.

2-(methyl((1-(naphthalen-1-yl)-1H-1,2,3-triazol-4-yl)methyl)amino)-BTZ (9). yield 60%; Solid, yellow color; ^{13}C NMR (151 MHz, CDCl$_3$) δ: 166.1, 163.5, 144.0, 141.9, 134.3, 133.7, 133.5, 130.7, 130.0 (q, *J* = 35.4 Hz), 128.5, 128.4, 128.1, 127.3, 126.7, 126.2, 125.1, 123.6, 122.5 (q, *J* = 273.1 Hz), 122.3, 46.8, 37.2; ^{1}H NMR (400 MHz, CDCl$_3$) δ: 9.10 (s, 1H), 8.77 (d, *J* = 1.6 Hz, 1H), 8.19 (s, 1H), 8.02 (d, *J* = 8.2 Hz, 1H), 7.95 (d, *J* = 8.0 Hz, 1H), 7.60 – 7.51 (m, 5H), 5.27 (s, 2H), 3.65 (s, 3H); HRMS-ESI (m/z) calcd [M+H]$^+$ for C$_{23}$H$_{16}$F$_3$N$_6$O$_3$S$^+$ 513.0951, found 513.0951.

2-(methyl((1-(thiophen-2-ylmethyl)-1H-1,2,3-triazol-4-yl)methyl)amino)-BTZ (10). yield 71%; Solid, yellow color; ^{13}C NMR (151 MHz, CDCl$_3$) δ: 166.1, 163.5, 144.0, 142.2, 135.8, 134.4, 133.6 (d, *J* = 2.6 Hz), 129.9 (q, *J* = 35.5 Hz), 128.5, 127.5, 127.4, 126.7, 126.1 (d, *J* = 2.8 Hz), 123.6, 122.5 (q, *J* = 273.3 Hz), 48.7, 46.5, 36.9; ^{1}H NMR (400 MHz, CDCl$_3$) δ: 9.11 (d, *J* = 1.6 Hz, 1H), 8.76 (d, *J* = 1.6 Hz, 1H), 7.77 (s, 1H), 7.31 (d, *J* = 4.8 Hz, 1H), 7.10 (d, *J* = 2.8 Hz, 1H), 7.03 – 6.93 (m, 1H), 5.67 (s, 2H), 5.10 (s, 2H), 3.49 (s, 3H); HRMS-ESI *(m/z)* calcd [M+H]$^+$ for C$_{18}$H$_{14}$F$_3$N$_6$O$_3$S$_2^+$ 483.0515, found 483.0512.

2-(methyl((1-(thiazol-4-ylmethyl)-1H-1,2,3-triazol-4-yl)methyl)amino)-BTZ (11). yield 43%; Solid, yellow color; ^{13}C NMR (151 MHz, CDCl$_3$) δ: 166.1, 163.5, 154.3, 150.2, 144.0, 142.2, 134.3, 133.6

(d, *J* = 3.3 Hz), 129.9 (q, *J* = 35.6 Hz), 126.7, 126.1 (d, *J* = 3.3 Hz), 124.3, 122.5 (d, *J* = 273.1 Hz), 118.1, 49.8, 46.5, 36.9; ^{1}H NMR (400 MHz, CDCl$_3$) *δ:* 9.11 (d, *J* = 2.0 Hz, 1H), 8.80 (s, 1H), 8.76 (d, *J* = 2.0 Hz, 1H), 7.91 (s, 1H), 7.32 (s, 1H), 5.68 (s, 2H), 5.12 (s, 2H), 3.49 (s, 3H); HRMS-ESI *(m/z)* calcd [M+H]$^+$ for C$_{17}$H$_{13}$F$_3$N$_7$O$_3$S$_2^+$ 484.0468, found 484.0467.

2-(((1-(4-fluorophenyl)-1H-1,2,3-triazol-4-yl)methyl)(methyl)amino)-BTZ **(12).** yield 66%; Solid, yellow color; ^{13}C NMR (151 MHz, CDCl$_3$) *δ:* 166.2, 163.6, 162.8 (d, *J* = 250.0 Hz), 143.9, 142.7, 134.3, 133.6 (d, *J* = 2.4 Hz), 133.1, 130.0 (q, *J* = 35.1 Hz), 126.7, 126.3 (d, *J* = 3.0 Hz), 122.7 (d, *J* = 8.4 Hz), 122.6, 122.5 (q, *J* = 273.1 Hz), 116.9 (d, *J* = 23.3 Hz), 46.6, 37.1; ^{1}H NMR (400 MHz, CDCl$_3$) *δ:* 9.12 (s, 1H), 8.78 (s, 1H), 8.26 (s, 1H), 7.69 (dd, *J* = 7.6, 4.4 Hz, 2H), 7.19 (t, *J* = 8.0 Hz, 2H), 5.20 (s, 2H), 3.57 (s, 3H); HRMS-ESI (m/z) calcd [M+H]$^+$ for C$_{19}$H$_{13}$F$_4$N$_6$O$_3$S$^+$ 481.0700, found 481.0692.

2-(((1-(3-fluorophenyl)-1H-1,2,3-triazol-4-yl)methyl)(methyl)amino)-BTZ **(13).** yield 59%; Solid, yellow color; ^{13}C NMR (151 MHz, CDCl$_3$) *δ:* 166.2, 163.6, 163.2 (d, *J* = 249.0 Hz), 143.9, 142.8, 138.0 (d, *J* = 9.5 Hz), 134.3, 133.7 (d, *J* = 2.4 Hz), 131.4 (d, *J* = 8.5 Hz), 132.9 (q, *J* = 35.5 Hz), 126.6, 126.2 (d, *J* = 2.8 Hz), 122.5 (q, *J* = 273.0 Hz), 122.4, 116.1, 116.0, 108.5 (d, *J* = 26.3 Hz), 46.7, 37.2; ^{1}H NMR (400 MHz, CDCl$_3$) *δ:* 9.13 (s, 1H), 8.78 (s, 1H), 8.30 (s, 1H), 7.56 – 7.47 (m, 3H), 7.14 (s, 1H), 5.18 (s, 2H), 3.58 (s, 3H); HRMS-ESI (m/z) calcd [M+H]$^+$ for C$_{19}$H$_{13}$F$_4$N$_6$O$_3$S$^+$ 481.0700, found:481.0701.

2-(((1-(2-fluorophenyl)-1H-1,2,3-triazol-4-yl)methyl)(methyl)amino)-BTZ **(14).** yield 53%; Solid,yellow color; ^{13}C NMR (151 MHz, CDCl$_3$) *δ:* 166.1, 163.6, 153.5 (d, *J* = 251.8 Hz), 143.9, 142.3, 134.2, 133.8 (d, *J* = 2.9 Hz), 130.7 (d, *J* = 6.8 Hz), 130.0 (q, *J* = 35.4 Hz), 126.7, 126.1, 125.4, 125.3, 125.1, 125.0, 122.5 (q, *J* = 273.2 Hz), 117.3 (d, *J* = 19.9 Hz), 46.5, 37.1; ^{1}H NMR (400 MHz, CDCl$_3$) *δ:* 9.12 (s, 1H), 8.76 (s, 1H), 8.29 (s, 1H), 7.88 (br, 1H), 7.44 (d, *J* = 5.2 Hz, 1H), 7.31 (t, *J* = 8.2 Hz, 2H), 5.23 (s, 2H), 3.56 (s, 3H); HRMS-ESI *(m/z)* calcd [M+H]$^+$ for C$_{19}$H$_{13}$F$_4$N$_6$O$_3$S$^+$ 481.0700, found 481.0696.

2-(((1-(3-chlorophenyl)-1H-1,2,3-triazol-4-yl)methyl)(methyl)amino)-BTZ **(15).** yield 49%; Solid, white color; ^{13}C NMR (151 MHz, CDCl$_3$) *δ:* 166.2, 163.6, 144.0, 142.9, 137.7, 135.8, 134.3, 133.7, 131.0, 130.0 (q, *J* = 35.9 Hz), 129.2, 126.7, 126.2, 122.6, 122.5 (q, *J* = 273.4 Hz), 121.0, 118.7, 46.8, 37.4; ^{1}H NMR (400 MHz, CDCl$_3$) *δ:* 9.14 (s, 1H), 8.78 (s, 1H), 8.25 (s, 1H), 7.77 (s, 1H), 7.60 (d, *J* = 7.3 Hz, 1H), 7.47–7.42 (m, 2H), 5.20 (s, 2H), 3.57 (s, 3H); HRMS-ESI (m/z) calcd [M+H]$^+$ for: C$_{19}$H$_{13}$ClF$_3$N$_6$O$_3$S$^+$ 497.0405, found:497.0407.

2-(((1-(3-bromophenyl)-1H-1,2,3-triazol-4-yl)methyl)(methyl)amino)-BTZ **(16).** yield 57%; Solid, white color; ^{13}C NMR (151 MHz, CDCl$_3$) *δ:* 166.2, 163.4, 144.0, 142.9, 137.8, 134.2, 133.6 (d, *J* = 2.4 Hz), 132.2, 131.2, 130.0 (q, *J* = 35.8 Hz), 126.5, 126.1 (d, *J* = 2.7 Hz), 123.8, 123.5, 122.5 (q, *J* = 273.0 Hz), 122.2, 119.1, 46.6, 37.2; ^{1}H NMR (400 MHz, CDCl$_3$) *δ:* 9.13 (s, 1H), 8.77 (s,1H), 8.26 (s, 1H), 7.93 (s, 1H), 7.65 (d, *J* = 7.6 Hz, 1H), 7.56 (d, *J* = 7.6 Hz, 1H), 7.38 (t, *J* = 7.8 Hz, 1H), 5.19 (s, 2H), 3.57 (s, 3H); HRMS-ESI (m/z) calcd [M+H]$^+$ for C$_{19}$H$_{13}$BrF$_3$N$_6$O$_3$S$^+$ 540.9900; 542.9879, found 540.9899; 542.9880.

2-(((1-(3-iodophenyl)-1H-1,2,3-triazol-4-yl)methyl)(methyl)amino)-BTZ **(17).** yield 70%; Solid,white color. ^{13}C NMR (151 MHz, CDCl$_3$) *δ:* 166.1, 163.6, 144.1, 142.8, 138.2, 137.6, 134.3, 133.7, 131.3, 130.0 (q, *J* = 35.2 Hz), 129.5, 126.6, 126.2 (d, *J* = 2.6 Hz), 122.5 (q, *J* = 273.2 Hz), 122.2, 119.8, 94.6, 46.6, 37.1; ^{1}H NMR (400 MHz, CDCl$_3$) *δ:* 9.13 (s, 1H), 8.77 (s, 1H), 8.24 (s, 1H), 8.10 (s, 1H), 7.76 (d, *J* = 7.6 Hz, 1H), 7.68 (d, *J* = 7.6 Hz, 1H), 7.22 (t, *J* = 7.6 Hz, 1H), 5.19 (s, 2H), 3.57 (s, 3H); HRMS-ESI (m/z) calcd [M+H]$^+$ for C$_{19}$H$_{13}$F$_3$IN$_6$O$_3$S$^+$ 588.9761, found: 588.9760.

2-(((1-(3-methoxyphenyl)-1H-1,2,3-triazol-4-yl)methyl)(methyl)amino)-BTZ **(18).** yield 57%; Solid, white color; ^{13}C NMR (151 MHz, CDCl$_3$) *δ:* 166.1, 163.5, 160.8, 144.1, 142.5, 137.9, 134.3, 133.7, 130.7, 130.0 (q, *J* = 35.6 Hz), 126.7, 126.2 (d, *J* = 2.6 Hz), 122.5 (q, *J* = 273.2 Hz), 122.3, 115.0, 112.6, 106.5, 55.8, 46.6, 37.1; ^{1}H NMR (400 MHz, CDCl$_3$) *δ:* 9.12 (s, 1H), 8.77 (s, 1H), 8.24 (s, 1H), 7.39 (t, *J* = 8.0 Hz, 1H), 7.30 (s, 1H), 7.23 (d, *J* = 7.8 Hz, 1H), 6.95 (d, *J* = 7.8 Hz, 1H), 5.20 (s, 2H), 3.86 (s, 3H), 3.57 (s, 3H); HRMS-ESI (m/z) calcd [M+H]$^+$ for C$_{20}$H$_{16}$F$_3$N$_6$O$_4$S$^+$ 493.0900, found 493.0900.

2-(methyl((1-(m-tolyl)-1H-1,2,3-triazol-4-yl)methyl)amino)-BTZ (19). yield 66%; Solid,white color; ^{13}C NMR (151 MHz, CDCl$_3$) *δ:* 166.2, 163.5, 144.0, 142.5, 140.2, 136.8, 134.4, 133.7 (d, *J* = 2.5 Hz), 130.0 (q, *J* = 35.6 Hz), 129.9, 129.7, 126.7, 126.2 (d, *J* = 2.7 Hz), 122.5 (q, *J* = 273.2 Hz), 122.3, 121.3, 117.8, 46.6, 37.1, 21.5; ^{1}H NMR (400 MHz, CDCl$_3$) *δ:* 9.13 (s, 1H), 8.77 (s, 1H), 8.22 (s, 1H), 7.53 (s, 1H), 7.48 (d, *J* = 8.0 Hz, 1H), 7.37 (t, *J* = 7.6 Hz, 1H), 7.23 (d, *J* = 7.6 Hz, 1H), 5.20 (s, 2H), 3.57 (s, 3H), 2.43 (s, 3H); HRMS-ESI (m/z) calcd [M+H]$^+$ for C$_{20}$H$_{16}$F$_3$N$_6$O$_3$S$^+$ 477.0951, found 477.0948.

2-(methyl((1-(3-(trifluoromethyl)phenyl)-1H-1,2,3-triazol-4-yl)methyl)amino)-BTZ (20). yield 65%; Solid, white color, ^{13}C NMR (151 MHz, CDCl$_3$) δ: 166.2, 163.7, 144.0, 143.1, 137.2, 134.3, 132.7 (q, J = 33.5 Hz), 130.7, 130.0 (q, J = 35.6 Hz), 129.6 (d, J = 4.0 Hz), 126.6, 126.2 (d, J = 3.3 Hz), 125.8, 123.8 (q, J = 272.8 Hz), 123.7, 123.4 (q, J = 272.7 Hz), 122.4, 117.8 (d, J = 3.7 Hz), 46.6, 37.2; ^{1}H NMR (400 MHz, CDCl$_3$) δ: 9.13 (s, 1H), 8.79 (s, 1H), 8.34 (s, 1H), 8.04 (br, 1H), 7.91 (br, 1H), 7.68 (d, J = 12.0 Hz, 2H), 5.20 (s, 2H), 3.58 (s, 3H); HRMS-ESI (m/z) calcd [M+H]$^+$ for C$_{20}$H$_{13}$F$_6$N$_6$O$_3$S$^+$ 531.0669, found 531.0669.

3-(4-((methyl(8-nitro-4-oxo-6-(trifluoromethyl)-4H-benzo[e][1,3]thiazin-2-yl)amino)methyl)-1H-1,2,3-triazol-1-yl)benzonitrile (21). yield 63%; Solid, white color. ^{13}C NMR (151 MHz, CDCl$_3$) δ: 166.1, 163.5, 143.9, 143.3, 137.5, 134.3, 133.7 (d, J = 2.30 Hz), 132.4, 131.2, 130.1 (q, J = 35.6 Hz), 126.6, 126.3 (d, J = 3.1 Hz), 124.5, 123.9, 122.5 (q, J = 273.3 Hz), 122.3, 117.4, 114.5, 46.7, 37.3; ^{1}H NMR (400 MHz, CDCl$_3$) δ: 9.13 (s, 1H), 8.77 (s, 1H), 8.36 (s, 1H), 8.10 (s, 1H), 7.98 (d, J = 7.60 Hz, 1H), 7.73 (d, J = 7.40 Hz, 1H), 7.66 (t, J = 7.80 Hz, 1H), 5.19 (s, 2H), 3.59 (s, 3H); HRMS-ESI (m/z) calcd [M+H]$^+$ for C$_{20}$H$_{13}$F$_3$N$_7$O$_3$S$^+$ 488.0747, found 488.074.

2-(((1-(3,4-difluorophenyl)-1H-1,2,3-triazol-4-yl)methyl)(methyl)amino)-BTZ (22). yield 61%; Solid,white color; ^{13}C NMR (151 MHz, CDCl$_3$) δ: 166.2, 163.6, 150.8 (dd, J = 252.2, 13.60 Hz), 150.5 (dd, J = 253.70, 13.6 Hz), 144.0, 143.0, 134.3 133.7 (d, J = 1.50 Hz),133.2, 130.1 (q, J = 36.24 Hz), 126.6, 126.2 (d, J = 3.0 Hz), 122.5 (q, J = 273.3 Hz), 122.5, 118.6 (d, J = 19.4 Hz), 116.7, 110.7 (d, J = 22.7 Hz), 46.7, 37.3; ^{1}H NMR (400 MHz, CDCl$_3$) δ: 9.13 (s, 1H), 8.78 (s, 1H), 8.26 (s, 1H), 7.68 – 7.64 (m, 1H), 7.44 (brs, 1H), 7.35 – 7.28 (m, 1H), 5.17 (s, 2H), 3.58 (s, 3H); HRMS-ESI (m/z) calcd [M+H]$^+$ for C$_{19}$H$_{12}$F$_5$N$_6$O$_3$S$^+$ 499.0606, found 499.0606.

2-(((1-(3,5-difluorophenyl)-1H-1,2,3-triazol-4-yl)methyl)(methyl)amino)-BTZ (23). yield 43%; Solid, white color. ^{13}C NMR (151 MHz, CDCl$_3$) δ: 166.2, 163.6, 163.55 (dd, J = 251.10, 13.7 Hz), 144.0, 143.1, 138.4 (d, J = 8.90 Hz), 134.3, 133.7 (d, J = 2.60 Hz), 130.1 (q, J = 35.40 Hz), 126.6, 126.3 (d, J = 3.0 Hz), 122.5 (q, J = 273.30 Hz), 122.4, 104.3 (d, J = 40.10 Hz), 104.2 (d, J = 30.50 Hz), 46.7, 37.3; ^{1}H NMR (400 MHz, CDCl$_3$) δ: 9.13 (s, 1H), 8.78 (s, 1H), 8.30 (s, 1H), 7.34 (d, J = 5.20 Hz, 2H), 6.89 (brs, 1H), 5.18 (s, 2H), 3.58 (s, 3H); HRMS-ESI (m/z) calcd [M+H]$^+$ for C$_{19}$H$_{12}$F$_5$N$_6$O$_3$S$^+$ 499.0606, found 499.0603.

2-(((1-(2,6-difluorophenyl)-1H-1,2,3-triazol-4-yl)methyl)(methyl)amino)-BTZ (24). yield 57%; Solid, white color; ^{13}C NMR (151 MHz, CDCl$_3$) δ: 166.1, 163.6, 156.9 (d, J = 256.70 Hz), 144.0, 141.8, 134.4, 133.7 (d, J = 2.10 Hz), 131.71 (t, J = 9.10 Hz), 130.0 (q, J = 35.50 Hz), 127.0, 126.7,126.2 (d, J = 3.00 Hz), 122.5 (q, J = 273.30 Hz), 115.1 (t, J = 15.10 Hz), 112.7 (d, J = 19.80 Hz), 46.6, 37.2; ^{1}H NMR (400 MHz, CDCl$_3$) δ: 9.11 (s, 1H), 8.77 (s, 1H), 8.10 (s, 1H), 7.50 – 7.47 (m, 1H), 7.12 (t, J = 8.4 Hz, 2H), 5.22 (s, 2H), 3.59 (s, 3H); HRMS-ESI (m/z) calcd [M+H]$^+$ for C$_{19}$H$_{12}$F$_5$N$_6$O$_3$S$^+$ 499.0606, found 499.0602.

2-(((1-(2,4-difluorophenyl)-1H-1,2,3-triazol-4-yl)methyl)(methyl)amino)-BTZ (25). yield 85%; Solid, white color. ^{13}C NMR (151 MHz, CDCl$_3$) δ: 166.0, 163.6, 162.7 (dd, J = 253.40, 10.9 Hz), 154.1 (dd, J = 254.70, 11.8 Hz), 144.0, 142.4, 134.3, 133.7 (d, J = 2.80 Hz), 130.0 (q, J = 35.50 Hz), 126.7,126.4 (d, J = 9.90 Hz), 126.1 (d, J = 2.60 Hz), 125.3 (d, J = 4.10 Hz), 122.5 (q, J = 273.60 Hz), 121.9 (d, J = 7.20 Hz), 112.7 (d, J = 22.40 Hz), 105.6 (dd, J = 78.5, 2.30 Hz), 46.5, 37.1; ^{1}H NMR (400 MHz, CDCl$_3$) δ: 9.13 (s, 1H), 8.78 (s, 1H), 8.26 (s, 1H), 7.88 – 7.82 (m, 1H), 7.08– 7.03 (m, 2H), 5.21 (s, 2H), 3.58 (s, 3H); HRMS-ESI (m/z) calcd [M+H]$^+$ for C$_{19}$H$_{12}$F$_5$N$_6$O$_3$S$^+$ 499.0606, found 499.0607.

2-(((1-(3,4-dichlorophenyl)-1H-1,2,3-triazol-4-yl)methyl)(methyl)amino)-BTZ (26). yield 65%; Solid, white color. ^{13}C NMR (151 MHz, CDCl$_3$) δ: 166.3, 163.6, 144.1, 143.1, 135.9, 134.2, 133.6 (d, J = 2.000 Hz), 133.4, 131.6, 130.1 (q, J = 35.3 Hz), 126.5, 126.3 (d, J = 3.0 Hz), 122.5 (q, J = 273.30 Hz), 122.5, 122.4, 122.3, 119.6, 46.7, 37.2; ^{1}H NMR (400 MHz, CDCl$_3$) δ: 9.14 (s, 1H), 8.78 (s, 1H), 8.29 (s, 1H), 7.91 (s, 1H), 7.59 (br, 2H)，5.18 (s, 2H), 3.57 (s, 3H); HRMS-ESI (m/z) calcd [M+H]$^+$ for C$_{19}$H$_{12}$Cl$_2$F$_3$N$_6$O$_3$S$^+$ 531.0015, found 531.0012.

2-(((1-(3-bromo-4-fluorophenyl)-1H-1,2,3-triazol-4-yl)methyl)(methyl)amino)-BTZ (27). yield 74%; solid, white color. Poor solubility to obtain a ^{13}C NMR. ^{1}H NMR (400 MHz, CDCl$_3$) δ: 9.13 (s, 1H), 8.78 (s, 1H), 8.25 (s, 1H), 7.98 (d, J = 3.2 Hz, 1H), 7.65 (d, J = 8.4 Hz, 1H), 7.29 (br, 1H), 5.18 (s, 2H), 3.58 (s, 3H); HRMS-ESI (m/z) calcd [M+H]$^+$ for C$_{19}$H$_{12}$BrF$_4$N$_6$O$_3$S$^+$ 558.9806, 560.9785, found 558.9794,560.9766.

2-(((1-(3-chloro-4-fluorophenyl)-1H-1,2,3-triazol-4-yl)methyl)(methyl)amino)-BTZ (28). 87%; Solid, white color. ^{13}C NMR (151 MHz, CDCl$_3$) δ: 166.3, 163.5, 158.2 (d, J = 252.2 Hz), 144.0, 143.0, 134.4, 133.6, 133.5, 130.1 (q, J = 34.7 Hz), 126.5, 126.3 (d, J = 3.0 Hz), 123.3, 122.8, 122.5, 122.5 (q, J = 273.3 Hz),

120.4 (d, J = 7.6 Hz), 117.8 (d, J = 22.7 Hz), 46.8, 37.3; ^{1}H NMR (400 MHz, CDCl$_3$) δ: 9.13 (s, 1H), 8.78 (s, 1H), 8.24 (s, 1H), 7.85 (d, J = 4.41 Hz, 1H), 7.61 (d, J = 7.19 Hz, 1H), 7.31 – 7.29 (m, 1H), 5.17 (s, 2H), 3.56 (s, 3H); HRMS-ESI *(m/z)* calcd [M+H]$^+$ for C$_{19}$H$_{12}$ClF$_4$N$_6$O$_3$S$^+$ 515.0311, found 515.0303.

2-(((1-(2,4-dichlorophenyl)-1H-1,2,3-triazol-4-yl)methyl)(methyl)amino)-BTZ (29). yield 72%; Solid, white color; ^{13}C NMR (151 MHz, CDCl$_3$) δ: 166.0, 163.4, 143.9, 141.9, 136.6, 134.4, 133.8 (d, J = 2.6 Hz), 133.4, 130.8, 130.0 (q, J = 35.6 Hz), 129.6, 128.5, 128.4, 126.6, 126.1, 122.5 (q, J = 273.0 Hz), 46.6, 37.3; ^{1}H NMR (400 MHz, CDCl$_3$) δ: 9.11 (d, J = 1.62 Hz, 1H), 8.77 (d, J = 1.62 Hz, 1H), 8.22 (s, 1H), 7.58 (d, J = 2.0 Hz, 1H), 7.52 (d, J = 8.8 Hz, 1H), 7.41 (dd, J = 8.4, 1.6 Hz, 1H), 5.21 (s, 2H), 3.58 (s, 3H); HRMS-ESI *(m/z)* calcd [M+H]$^+$ for C$_{19}$H$_{12}$Cl$_2$F$_3$N$_6$O$_3$S$^+$ 531.0015, found 531.0015.

2-(((1-(3,5-dichlorophenyl)-1H-1,2,3-triazol-4-yl)methyl)(methyl)amino)-BTZ (30). yield 75%; Solid, white color. ^{13}C NMR (151 MHz, CDCl$_3$) δ: 166.2, 163.7, 144.0, 143.1, 138.1, 136.5, 134.2, 133.7 (d, J = 2.8 Hz), 130.1 (q, J = 35.2 Hz), 129.1, 126.6, 126.2 (d, J = 2.7 Hz), 122.6 (q, J = 273.0 Hz), 122.2, 119.1, 46.6, 37.2; ^{1}H NMR (400 MHz, CDCl$_3$) δ: 9.13 (d, J = 1.6 Hz, 1H), 8.78 (d, J = 1.2 Hz, 1H), 8.28 (s,1H), 7.68 (d, J = 1.6 Hz, 2H), 7.42 (s, 1H), 5.20 (s, 2H), 3.56 (s, 3H); HRMS-ESI *(m/z)* calcd [M+H]$^+$ for C$_{19}$H$_{12}$Cl$_2$F$_3$N$_6$O$_3$S$^+$ 531.0015, found 531.0016.

2-(methyl((2-phenyloxazol-4-yl)methyl)amino)-BTZ (31). Solid, white color; ^{1}H NMR indicates 3:1 atropisomeric ratio through the integral value of −CH$_2$ protons and the oxazole – CH protons; ^{13}C NMR (151 MHz, CDCl$_3$) δ: 166.2, 166.1, 162.1, 144.0, 137.6, 136.2, 134.4, 133.7, 130.8, 129.9 (q, J = 35.40 Hz), 129.0, 126.8, 126.7, 126.1, 122.5 (q, J = 273.3 Hz), 116.3, 46.9, 37.1; ^{1}H NMR (400 MHz, CDCl$_3$) δ: 9.15 (s, 1H), 8.76 (s, 1H), 8.01 (br, 2H), 7.85 (s, 0.75H, major), 7.77 (s, 0.25H, minor), 7.45 (br, 3H), 5.06 (s, 1.5H, major), 4.88 (s, 0.5H, minor), 3.57 (s, 3H); HRMS-ESI *(m/z)* calcd [M+H]$^+$ for C$_{20}$H$_{14}$F$_3$N$_4$O$_4$S$^+$ 463.0682, found 463.0683.

2-(((2-(4-fluorophenyl)oxazol-4-yl)methyl)(methyl)amino)-BTZ (32). Solid, white; ^{1}H NMR indicates 3:1 atropisomeric ratio through the integral value of −CH$_2$ protons and the oxazole −CH protons; ^{13}C NMR (151 MHz, CDCl$_3$) δ: 166.1, 164.3 (d, J = 252.4 Hz), 163.5, 161.2, 144.0, 137.6, 136.2, 134.4, 133.7, 129.9 (d, J = 35.6 Hz), 128.7 (d, J = 7.9 Hz), 126.7, 126.1, 123.6, 122.5 (d, J = 273.0 Hz), 116.0 (d, J = 22.1 Hz), 46.9, 37.1; ^{1}H NMR (400 MHz, CDCl$_3$) δ: 9.09 (s, 1H), 8.72 (s, 1H), 7.96 (br, 2H), 7.78 (s, 0.75H, major), 7.72 (s, 0.25H, minor), 7.09 (t, J = 7.5 Hz, 2H), 4.99 (s, 1.5H, major), 4.81 (s, 0.5H, minor), 3.51 (s, 3H); HRMS-ESI *(m/z)* calcd [M+H]$^+$ for C$_{20}$H$_{13}$F$_4$N$_4$O$_4$S$^+$ 481.0588, found 481.0586.

2-(((2-(3-fluorophenyl)oxazol-4-yl)methyl)(methyl)amino)-BTZ (33). A white solid; ^{1}H NMR indicates 3:1 atropisomeric ratio through the integral value of −CH$_2$ protons and the oxazole −CH protons; ^{13}C NMR (151 MHz, CDCl$_3$) δ: 166.1, 163.5, 160.1 (d, J = 256.0 Hz), 158.4, 138.0, 137.6, 136.2, 134.4, 133.7, 132.4 (d, J = 7.2 Hz), 129.9 (d, J = 35.6 Hz), 129.7, 128.9, 126.7, 126.1, 124.5, 122.5 (q, J = 273.2 Hz), 117.0 (d, J = 21.2 Hz), 46.8, 37.1; ^{1}H NMR (400 MHz, CDCl$_3$) δ: 9.09 (s, 1H), 8.73 (s, 1H), 7.95 (s, 1H), 7.86 (s, 0.75H, major), 7.79 (s, 0.25H, minor), 7.41 (br, 1H), 7.21 – 7.10 (m, 2H), 5.04 (s, 1.5H, major), 4.85 (s, 0.5H, minor), 3.52 (s, 3H); HRMS-ESI *(m/z)* calcd [M+H]$^+$ for C$_{20}$H$_{13}$F$_4$N$_4$O$_4$S$^+$ 481.0588, found 481.0587.

2-(methyl((2-phenylthiazol-4-yl)methyl)amino)-BTZ (34). Solid, white color; ^{1}H NMR indicates 3:1 atropisomeric ratio through the integral value of −CH$_2$ protons; ^{13}C NMR (151 MHz, CDCl$_3$) δ: 168.7, 166.2, 163.5, 151.1, 144.0, 134.5, 133.7, 130.4, 129.8 (q, J = 35.4 Hz), 129.1, 126.9, 126.6, 126.1, 122.5 (q, J = 273.3 Hz), 118.2, 116.8, 50.7, 37.2; ^{1}H NMR (400 MHz, CDCl$_3$) δ: 9.13 (s, 1H), 8.76 (d, J = 1.9 Hz, 1H), 7.96 – 7.88 (m, 2H), 7.44 – 7.41 (m, 4H), 5.22 (s, 1.5H , major), 5.03 (s, 0.5H , minor), 3.57 (s, 3H); HRMS-ESI *(m/z)* calcd [M+H]$^+$ for C$_{20}$H$_{14}$F$_3$N$_4$O$_3$S$_2$$^+$ 479.0454, found 479.0451.

2-(((2-(3-fluorophenyl)thiazol-4-yl)methyl)(methyl)amino)-BTZ (35). Solid, white color; ^{1}H NMR indicates 3:1 atropisomeric ratio through the integral value of −CH$_2$ protons and the thiazole −CH protons; ^{13}C NMR (151 MHz, CDCl$_3$) δ: 166.2, 163.6, 160.1 (d, J = 253.5 Hz), 150.1, 144.0, 134.5, 133.7, 131.4 (d, J = 7.2 Hz), 129.8 (q, J = 34.6 Hz), 129.1, 128.8, 126.8, 126.6, 126.1, 124.7, 122.5 (q, J = 272.8 Hz), 119.6 (d, J = 7.3 Hz), 116.3 (d, J = 21.8 Hz), 50.7, 37.2; ^{1}H NMR (400 MHz, CDCl$_3$) δ: 9.13 (s, 1H), 8.76 (s, 1H), 8.24 (br, 1H), 7.91 (s, 0.75H,major), 7.52 (s, 0.25H,minor), 7.42 (br, 2H), 7.23 – 7.16(m, 1H), 5.24 (s, 1.5H, major), 5.06 (s, 0.5H, minor), 3.57 (s, 3H); HRMS-ESI *(m/z)* calcd [M+H]$^+$ for C$_{20}$H$_{13}$F$_4$N$_4$O$_3$S$_2$$^+$ 497.0360, found 497.0358.

2-(((2-(4-fluorophenyl)thiazol-4-yl)methyl)(methyl)amino)-BTZ (36). Solid, white color; ^{1}H NMR indicates 2:3 atropisomeric ratio through the integral value of −CH$_2$ protons and the thiazole

−CH protons; ^{13}C NMR (151 MHz, CDCl$_3$) δ: 166.3, 163.5, 162.3 (d, J = 279.0 Hz), 151.1, 144.0, 134.5, 133.7, 130.4, 129.8 (q, J = 35.4 Hz), 129.1, 126.8, 126.7, 126.1, 122.5 (d, J = 273.1 Hz), 118.2, 116.8, 50.7, 37.2; ^{1}H NMR (400 MHz, DMSO-d_6) δ: 8.86 (s, 1H), 8.82 (s, 1H), 7.92 (br, 2H), 7.80 (s, 0.4 H, minor), 7.63 (s, 0.6 H, major), 7.49 (br, 2H), 5.18 (s, 1.2H, major), 5.14 (s, 0.8H, minor), 3.47 – 3.41 (m, 3H); HRMS-ESI *(m/z)* calcd [M+H]$^+$ for C$_{20}$H$_{13}$F$_4$N$_4$O$_3$S$_2^+$ 497.0360, found 497.0358.

2-(methyl((5-phenyl-1,3,4-oxadiazol-2-yl)methyl)amino)-BTZ (37). Solid, yellow color; ^{13}C NMR (151 MHz, CDCl$_3$) δ: 166.2, 166.1, 164.8, 160.8, 144.0, 133.9 (d, J = 2.8 Hz), 132.2, 130.2 (q, J = 35.49 Hz), 129.2, 127.1, 126.5, 126.2 (d, J = 3.2 Hz), 123.2, 122.3 (q, J = 274.0 Hz), 45.2, 36.7; ^{1}H NMR (400 MHz, CDCl$_3$) δ: 9.15 (s, 1H), 8.82 (s, 1H), 8.03 (d, J = 7.60 Hz, 2H), 7.56 – 7.46 (m, 3H), 5.43 (s, 2H), 3.54 (s, 3H); HRMS-ESI (m/z) calcd [M+H]$^+$ for C$_{19}$H$_{13}$F$_3$N$_5$O$_4$S$^+$ 464.0635, found 464.0632.

2-(((5-(3-fluorophenyl)-1,3,4-oxadiazol-2-yl)methyl)(methyl)amino)-BTZ (38). Solid, yellow color; ^{13}C NMR (151 MHz, CDCl$_3$) δ: 166.1,165.6, 164.9, 162.8, 160.2 (d, J = 259.0 Hz), 144.1, 134.2 (d, J = 5.4 Hz), 133.8, 130.3 (q, J = 35.8 Hz), 130.0, 126.6, 126.4 (d, J = 3.2 Hz), 124.9 (d, J = 3.1 Hz), 122.4 (q, J = 273.6 Hz), 117.2 (d, J = 20.8 Hz), 111.9 (d, J = 14.2 Hz), 110.2, 45.3, 37.0; ^{1}H NMR (400 MHz, CDCl$_3$) δ: 9.14 (s, 1H), 8.81 (s, 1H), 8.03 (t, J = 7.0 Hz, 1H), 7.55 (dd, J = 6.8 Hz , J = 12.4 Hz , 1H), 7.31 – 7.21 (m, 2H), 5.44 (s, 2H), 3.56 (s, 3H); HRMS-ESI (m/z) calcd [M+H]$^+$ for C$_{19}$H$_{12}$F$_4$N$_5$O$_4$S$^+$ 482.0541, found 482.0541.

2-(((5-(4-fluorophenyl)-1,3,4-oxadiazol-2-yl)methyl)(methyl)amino)-BTZ (39). Solid, yellow color; ^{13}C NMR (151 MHz, CDCl$_3$) δ: 166.1, 165.3, 165.2 (d, J = 254.1 Hz), 165.0, 161.0, 144.2, 134.0 (d, J = 2.9 Hz), 130.3 (q, J = 35.5 Hz), 129.6 (d, J = 8.9 Hz), 126.6, 126.4 (d, J = 3.2 Hz), 122.4 (q, J = 273.6 Hz), 119.7, 116.7 (d, J = 22.3 Hz), 45.2, 37.0; ^{1}H NMR (400 MHz, CDCl$_3$) δ: 9.14 (s, 1H), 8.82 (s, 1H), 8.04 – 8.01 (m, 2H), 7.18 (t, J = 8.0 Hz, 2H), 5.41 (s, 2H), 3.55 (s, 3H); HRMS-ESI (m/z) calcd [M+H]$^+$ for C$_{19}$H$_{12}$F$_4$N$_5$O$_4$S$^+$ 482.0541, found 482.0541.

2-(methyl((5-phenyl-1,3,4-thiadiazol-2-yl)methyl)amino)-BTZ (40). Solid, white color; ^{13}C NMR (151 MHz, CDCl$_3$) δ: 171.2, 165.8, 164.0, 162.1, 134.0, 133.9 (d, J = 3.2 Hz), 131.6, 130.3 (q, J = 35.6 Hz), 129.8, 129.4, 128.1, 126.6, 126.4 (d, J = 3.5 Hz), 122.4 (q, J = 273.2 Hz), 110.0, 49.8, 36.9; ^{1}H NMR (400 MHz, CDCl$_3$) δ: 9.17 (s, 1H), 8.82 (s, 1H), 7.93 (d, J = 6.8 Hz, 2H), 7.49 – 7.45 (m, 3H), 5.44 (s, 2H), 3.54 (s, 3H); HRMS-ESI (m/z) calcd [M+H]$^+$ for C$_{19}$H$_{13}$F$_3$N$_5$O$_3$S$_2^+$ 480.0406, found 480.0405.

2-(((5-(3-fluorophenyl)-1,3,4-thiadiazol-2-yl)methyl)(methyl)amino)-BTZ (41). Solid, yellow color; ^{13}C NMR (151 MHz, CDCl$_3$) δ: 170.0, 165.8, 164.1, 163.7, 159.7 (d, J = 253.0 Hz), 144.1, 133.9 (d, J = 3.0 Hz), 133.1 (d, J = 8.4 Hz), 130.3 (q, J = 35.6 Hz), 129.2, 126.7, 126.3 (d, J = 3.0 Hz), 125.1, 122.3 (q, J = 273.1 Hz), 118.1 (d, J = 7.7 Hz), 116.6 (d, J = 21.7 Hz), 49.5, 36.8; ^{1}H NMR (400 MHz, CDCl$_3$) δ: 9.17 (s, 1H), 8.81 (s, 1H), 8.35 (t, J = 6.8 Hz, 1H), 7.50 (dd, J = 5.6 Hz, J = 11.2 Hz, 1H), 7.30 (t, J = 7.19 Hz, 1H), 7.20 (t, J = 9.6 Hz, 1H), 5.50 (s, 2H), 3.54 (s, 3H); HRMS-ESI (m/z) calcd [M+H]$^+$ for C$_{19}$H$_{12}$F$_4$N$_5$O$_3$S$_2^+$ 498.0312, found 498.0314.

2-(((5-(4-fluorophenyl)-1,3,4-thiadiazol-2-yl)methyl)(methyl)amino)-BTZ (42). Solid, yellow color; ^{13}C NMR (151 MHz, CDCl$_3$) δ: 170.1, 165.7, 164.6 (d, J = 253.1 Hz), 163.9, 162.1, 144.1, 134.0 (d, J = 3.0 Hz), 130.3, 130.1 (d, J = 8.7 Hz), 123.0 (q, J = 35.4 Hz), 126.5, 126.3 (d, J = 3.2 Hz), 126.2, 122.3 (q, J = 273.2 Hz), 116.5 (d, J = 22.1 Hz), 49.9, 37.0; ^{1}H NMR (400 MHz, CDCl$_3$) δ: 9.17 (s, 1H), 8.82 (s, 1H), 8.02 – 7.86 (m, 2H), 7.14 (t, J = 8.0 Hz, 2H), 5.42 (s, 2H), 3.53 (s, 3H); HRMS-ESI (m/z) calcd [M+H]$^+$ for C$_{19}$H$_{12}$F$_4$N$_5$O$_3$S$_2^+$ 498.0312, found 498.0317.

2.3. MIC Determination

The MIC against replicating *M. tuberculosis* against H37Rv were determined using microplate alamar blue assay (MABA), as previously reported[9]. Compound PBTZ169 was employed as a positive control. At 37°C, *M. tuberculosis* H37Rv (ACTT 25618) strains were cultured in Difco Middlebrook 7H9 Broth (Seebio), with 0.2% (v/v) glycerol, 0.05% Tween 80, and 10% (v/v) albumin-dextrose-catalase (Seebio) (7H9-ADC-TG) to grow into late log phase (70-100 Klett units), then centrifuged, washed twice, and resuspended in phosphate-buffered saline. All tested compound stock solutions were initially prepared in DMSO, then serially diluted in two-fold in 7H9-ADC-TG in a volume of 100 µL in 96-well clear-bottom microplates (BD), then added the bacterial culture suspension in 100 µL containing 2 × 10^5 CFU) to yield a final testing volume of 200 µL The tested

compound concentration range was 2 to 0.002 μg/mL. The plates containing the corresponding compounds were incubated at 37 °C. On day 7, 20 μL of alamar blue and 50 μL 5% Tween 80 were added to all wells. After incubation at 37 °C for 16-24 h, the fluorescence signal was read at an excitation of 530 nm and an emission of 590 nm. The MIC was defined as the lowest concentration resulting in a reduction in fluorescence of ≥90% relative to the mean of replicate bacterium-only controls.

2.4. Compound IC_{50} Determination

The recombinant *M. tuberculosis* DprE1 enzyme was produced in *E. coli*, as previously reported. Enzymatic activity was assayed using a Amplex Red/peroxidase coupled assay at 30 °C. Briefly, DprE1 (0.15 μM) was incubated in 20 mM glycylglycine pH 8.5, containing 0.05 mM Amplex Red, and 0.35 μM horseradish peroxidase; the reaction was started by addition of 0.5 mM FPR, and monitored by measuring the generation of resorufin at 572 nm (ε=54,000 M^{-1} cm^{-1}) . For inhibition studies, each compound (dissolved in DMSO) was firstly assayed at a final concentration of 20 μM, using DMSO as negative and PBTZ169 as positive control. Compounds displaying less than 20% of residual activity at 20 μM were further investigated, through the determination of IC_{50} and the analysis of kinetic inactivation of DprE1 as previously reported. $A_{[I]} = A_{[0]} \times \left(1 - \frac{[I]}{[I]+IC_{50}}\right)$

where $A_{[I]}$, $A_{[0]}$ is the initial activity of DprE1 at inhibitor concentration [I], or the initial activity in the absence of inhibitor, respectively.

2.5. Metabolic labeling of M. tuberculosis H37Rv

M. tuberculosis were incubated in 7H9 media supplemented with Tween 80 and ADC at 37 °C with shaking until OD_{600} 0.9. Radiolabelling with [^{14}C]-acetate [specific activity: 110 mCi/mmol, American Radiolabeled Chemicals, Inc.] in the final concentration of 1 μCi/mL was performed as described[10], for 24 hrs, in the volume of 100 μL at concentrations 10 x MIC, 100 x MIC of the target compounds. The lipids were extracted with 1.5 mL of $CHCl_3$/CH_3OH (2:1) by incubation at 65 °C for 3 hours. Following the biphasic Folch wash (2 x), the samples were analysed on TLC Silica gel 60 F_{254} plates in the solvent $CHCl_3$/CH_3OH/H_2O (20:4:0.5, v/v) and the radiolabeled lipids were visualized by Amersham Typhoon 5 phosphorimager (GE Healthcare).

2.6. Liver Microsomal Metabolic Stability Test

The compounds metabolic stability were determined in human liver microsomes. A solution of microsomes (0.2 mg/mL) containing the compounds (1.0 mM), NADPH (1 mM), phosphate buffer (100 mM, pH 7.4) were prepared. Pre-incubation at 37 °C for 10 min. Addition of 50 uL, 5 mM NADPH to initiate the reaction. At 5, 15, 30, 60, or 120 min, 30 uL of reaction solution was taken out and quenched with 300 uL internal standard tolbutamide(10 ng/mL) in cold CH_3CN. The mixture was centrifuged at 6000 rpm for 15 min at 4 °C. Then, 100 μL supernatant was diluted with 100 uL ultrapure water (Millipore, ZMQS50F01). The solution was analyed by LC/MS analysis.

2.7. Pharmacokinetic Study in Mice

Animal Care and Welfare Committee of Shanghai Institute of Materia Medica, Chinese Academy of Sciences approved all animal protocols. All animal programs are in compliance with the Guide for the Care and Use of Laboratory Animals issued by Shanghai Association on Laboratory Animal Care (SALAC). SPF male ICR mice weighing 25–27 g were divided into two groups，three mice in each group. The tested compound were administrated in oral and intravenous injection, separately. The compound was oral dosed at 5 mg/kg at a concentration as 1.0 mg/mL and intravenously (i.v.) dosed 2 mg/kg as 0.4 mg/mL. The compound was co-dissolved by using 0.5% carboxymethyl cellulose for p.o. administration, and 10% DMSO/40%PEG400/40% water was used for i.v. administration, respectively. After oral dosing or i.v. administration, the blood sampled at 5, 15, 30 min, 1, 2, 4, 7, 24 h. The sample plasma was harvested and stored at -80 °C for analysis. Based on noncompartmental

analysis (Pharsight Corporation, Mountain View), the pharmacokinetic data were analyed using WinNonlin software version 6.3.

2.8. In vivo Efficacy Study

Animal work was approved by the Bioethics Committee at the Research Center of Biotechnology of RAS (Protocol N◦22/1, February 11, 2022) and was carried out according to the corresponding guidelines for animal use. Female 2-month-old BALB/c mice were kept in cages with a floor area of 960 cm^2 and a height of 12 cm (North Kent Plastic Cages, UK), in a special room with separate supply and exhaust ventilation without recirculation, equipped with a HEPA filter at the outlet, under standard conditions (natural light/dark cycle, air temperature 21–22°C, relative humidity 50%, 15-fold air exchange rate). Water and standard rodent compound feed (PK-120; Laboratorkorm, Moscow, Russia) were provided *at libitum*.

After 6 days of adaptation, mice were randomized into groups (n = 6) and inoculated with 0.2 μL of a suspension containing 3.6×10^6 CFU of virulent *M. tuberculosis* strain H37Rv in PBS containing 0.0027 M KCl and 0.138 M NaCl per mouse intravenously in the lateral tail vein using a sterile 0.5 mL-tuberculin syringe with a 28G 1/2″ needle (ISO-Med, Inc, Corona, CA).

Solutions of test compounds were prepared in PBS buffer (pH 7.0, 50 mM) containing PEG-400 (40%) as a solubilizer and dispersed in an ultrasonic bath. One week after *Mtb* infection, the compounds were administered once a day intragastrically using a syringe pump (Harvard Apparatus, Holliston, MA, USA). Treatment was continued for 4 weeks, except weekends. Euthanasia was performed by dislocation of the cervical vertebrae.

To determine the number of Mtb CFU, the lungs from animals of each group were homogenized using a YellowlineD1 25 basic homogenizer (IKA-WERKE, Staufen im Breisgau, Germany). 10-fold Serial dilutions of the initial suspension in saline was prepared, 100 μL of each dilution was placed on a Petri dish with Dubos agar, and incubated for 21 days. The number of colonies per plate was then counted and the number of CFU of Mtb/lung was determined. The obtained quantitative data CFU Mtb/lung were converted to log10.

Statistical analysis was performed using an MS Office Excel software. Mean value (M), standard deviation (SD), statistical significance (p) was evaluated at 95% confidence interval by Student's t-test.

3. Results

3.1. Chemistry

Chemical Synthesis

Compounds **1–30** were prepared as shown in Scheme 1. The intermediate **43** and **45** was prepared according to published methods[11]. Click chemistry between **45** and corresponding azide using $CuSO_4$ and sodium ascorbate in $EtOH/H_2O$ gave final compounds **1–30**.
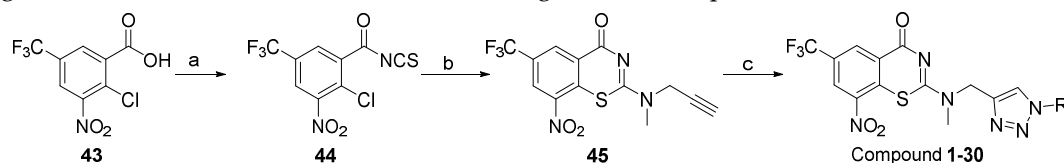
Reagents and conditions: (a) oxalyl chloride, a drop of DMF, DCM, 0.5 h; then NH_4SCN, DCM/CH_3COCH_3 = 5:1, 1.0 h, rt; (b) *N*-methylpropagyl amine, 2.5 h, DCM, yield 65%; (c) corresponding azide R-N_3, $CuSO_4$, K_2CO_3, sodium ascorbate, $EtOH/H_2O$, rt, 16 h, yield: 40–68%.
Scheme 1. Synthesis of compound **1–30**.

Compounds **31–36** were prepared as shown in Scheme 2. The reaction intermediates **46a**–**c** and **47a**–**c** were prepared according to the published procedure[11]. The final cyclization reaction between **44** and the above intermediates afforded compounds **31–36** in medium yield.
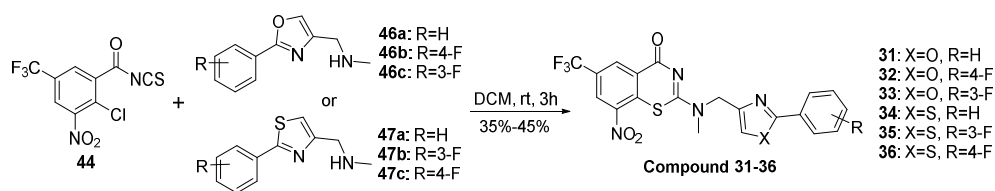
Scheme 2. Synthesis of compounds **31–36**.

Compounds **37**–**43** were prepared as shown in **Scheme 3**. The reaction intermediates **48a**–**c** and **49a**–**c** were prepared according to the published procedure[11]. The final cyclization reaction of **44** with the above intermediates provided the target compounds **37**–**42** in 30%–50% yields.
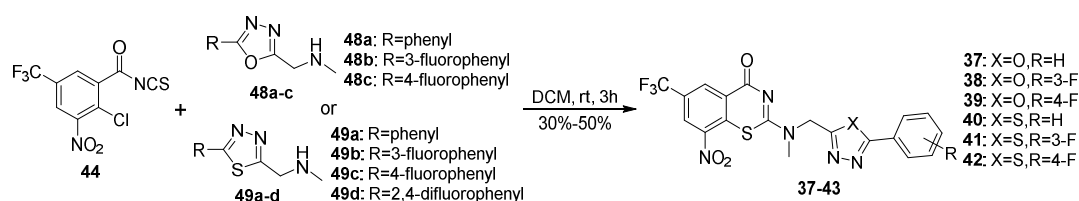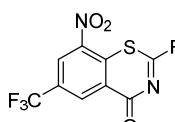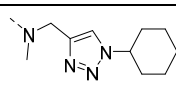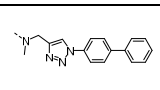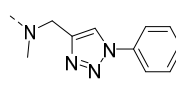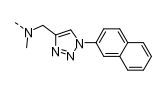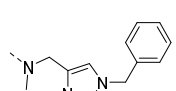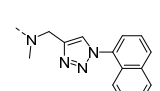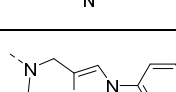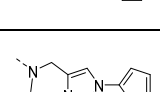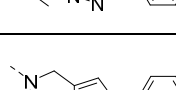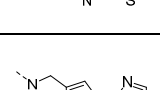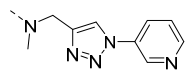
Scheme 3. Synthesis of compound **31–36**.

3.2. MIC Determination and Structure Activity Relationship

The compound antimycobacterial activity was performed as previously described[11]. The triazole moiety has been widely used in drug molecules and regarded as a privileged motif[12]. More importantly, the facile click chemistry to construct triazole is readily achieved through the reaction between a terminal alkyne and an azide, the 1,2,3-triazole linker compounds **1–11** displayed MIC 4–237 ng/mL, The MIC values are shown in **Table 1**. Specifically, the *N*-cyclohexyltriazole **1** exhibited MIC 16 ng/mL against Mtb H37Rv. the *N*-phenyltriazole **2** was 4–fold more potent, with MIC 4 ng/mL. Reduced activities were recorded for *N*-benzyltriazole **3** and compound **4**. Notably, all compounds showed ~5–fold activity improvement as compared to our previously reported 6-methanesulfonyl counterparts[11].

Table 1. Antitubercular activity of compounds **1–11** against Mtb H37Rv.
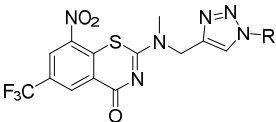
entry	R	MIC (ng/mL)	entry	R	MIC (ng/mL)
1		15	**7**		237
2		4	**8**		29
3		15	**9**		111
4		16	**10**		25
5		22	**11**		153
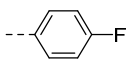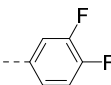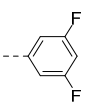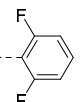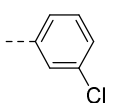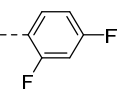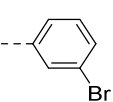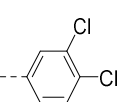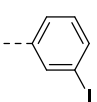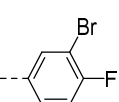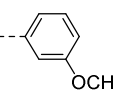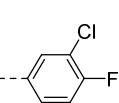
6		79	**PBTZ169**		0.2
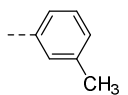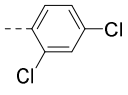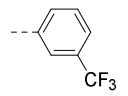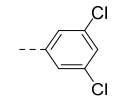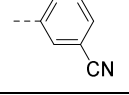
Having profiled the tail position, we then defined the phenyl group and intended to further investigate the substitute effect at the phenyl ring (**Table 2**), aiming to obtain compounds with higher potency and improved physiochemical properties than compound **2**. Replacement of one or more hydrogens with a fluorine atom is a commonly employed tactic to elevate the compounds ADME properties[13]. Thus, the analogs **12**, **13** and **14** with one fluorine atom at different position were prepared. The *meta*-F substituted compound **13**, MIC 4.0 ng/mL, had the highest potency among these three compounds, compounds **12** and **14** had MIC 6 and13 ng/mL, respectively.

We then explored the *meta*- position by introducing an electron withdrawing or donating group. Within this frame, compounds **15–21** were generated. Unfortunately, none of them exhibited activity improvement, higher MIC values of 7–101 ng/mL were recorded. Specifically, gradual activity loss was observed from chloro- to bromo- and iodo-. Other groups like methyl, methoxyl, and trifluoromethyl substitution also diminished the Mtb growth inhibition activity. The meta-cyano substituted compound **21** showed the weakest activity. Thus, our optimization choice was turned to phenyl di-substitution, generating compounds **22–29**. The di-substitution strategy also failed to provide compounds with further potency increase. Among these compounds, the three difluoro-substituted compounds **22**, **23** and **24** showed MICs lower than 10 ng/mL. In contrast, the 2,5-difluoro substituted compound **24** displayed MIC 129 ng/mL.

Table 2. Antitubercular activity of compounds **12–30** against Mtb H37Rv.
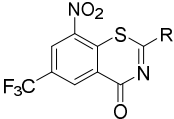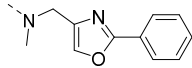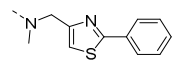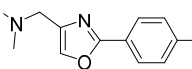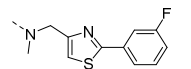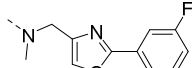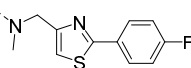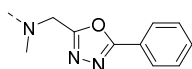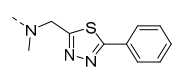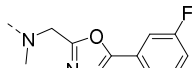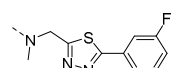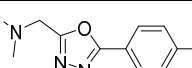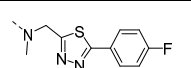
entry	R	MIC (ng/mL)	entry	R	MIC (ng/mL)
12		6	**22**		7
13		4	**23**		8
14		13	**24**		129
15		7	**25**		7
16		30	**26**		19
17		78	**27**		31
18		59	**28**		15

19	(3-CH₃-phenyl)	29	29	(2,4-dichlorophenyl)	12
20	(3-CF₃-phenyl)	21	30	(3,5-dichlorophenyl)	25
21	(3-CN-phenyl)	101	**PBTZ 169**		0.2

Having established that the triazole linker and the phenyl attachment could drop down MICs to less than 10 ng/mL, we next replaced this linker with its bioisosters. Other five-member heterocycles like oxazole, thiazole, oxadiazole or thiodiazole are considered as suitable surrogates of triazole[14]. We postulated that replacement of triazole with the heterocycles likely generates analogs with different physiochemical properties. Compounds **31**–**42** were designed and synthesized using various linkers (**Table 3**). It was interesting that the oxazole linker compounds **31–33** and the three 1,3,4-oxadiazole compounds **37–39** displayed antitubercular activity higher than or comparable to compound **2**. The MIC of compound **34** with a thiazole linker was 7 ng/mL, while compounds **35** and **36** with substituted phenyl attachment exhibited decreased activity (MIC 16 and 17 ng/mL, respectively). Similarly, the 1,3,4-thiodiazole-linked compounds **40–42** displayed higher MIC values.

Table 3. Antitubercular activity of compounds **31–42** against Mtb H37Rv.

entry	R	MIC (ng/mL)	entry	R	MIC (ng/mL)
31	(oxazole-phenyl)	3	**34**	(thiazole-phenyl)	7
32	(oxazole-4-F-phenyl)	3	**35**	(thiazole-3-F-phenyl)	16
33	(oxazole-3-F-phenyl)	10	**36**	(thiazole-4-F-phenyl)	17
37	(1,3,4-oxadiazole-phenyl)	3	**40**	(1,3,4-thiadiazole-phenyl)	16
38	(1,3,4-oxadiazole-3-F-phenyl)	3	**41**	(1,3,4-thiadiazole-3-F-phenyl)	12
39	(1,3,4-oxadiazole-4-F-phenyl)	3	**42**	(1,3,4-thiadiazole-4-F-phenyl)	13

3.3. DprE1 Inhibition Activity

The above compounds with various linkers were selected based on their MIC values to test potential on-target inhibitory activity of the Mtb DprE1 enzyme. Following a previously reported assay method[9], all of the compounds inhibited the DprE1 activity, with the IC_{50} values ranging from 0.02 to 7.2 μM (**Figure 2**, and Supplementary Table S1). Compounds with low MICs accordingly exhibited lower IC_{50} values as observed in the DprE1 inhibitory assays. For example, compounds **2**, **31**, **34**, and **37** had the IC_{50} values of 0.02–0.75 μM, and the least potent compound **24** displayed an

IC$_{50}$ of 7.2 μM. As a comparison, the positive control PBTZ169 displayed IC$_{50}$ 0.009 μM, consistent with the value reported in literature[6].
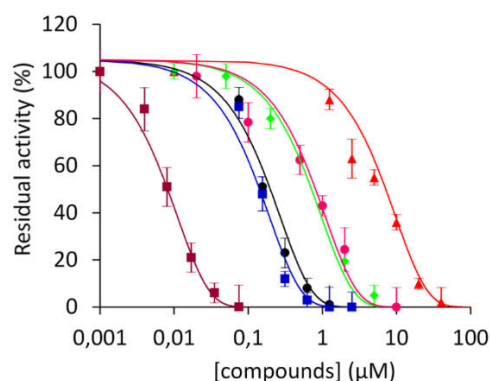
Figure 2. IC$_{50}$ determination of compounds **2** (●), **24** (▲), **31** (■), **34** (◆), **37** (●) and **PBTZ169** (■), against the DprE1 activity.

3.4. Compound–mediated Cell Wall Inhibition of Mtb

The ability of the compounds **2** and **37** to inhibit the DprE1 enzyme in Mtb H37Rv was examined by [^{14}C]-acetate metabolic labeling, as described before (**Figure 3**)[10]. Analysis of the extractable lipids from radiolabeled bacteria by TLC points out to similar profiles for PBTZ169 and the two tested inhibitors, suggesting the same mechanism of action. The cultures treated with the inhibitors accumulated trehalose monomycolates (TMM) and trehalose dimycolates (TDM) compared to the control bacteria, which indicates interference with the build-up of the mycobacterial cell wall core. DprE1 inhibition causes deficiency in the synthesis of arabinan chains serving as attachment sites for mycolic acids, which then incorporate to soluble lipids, TMM and TDM.
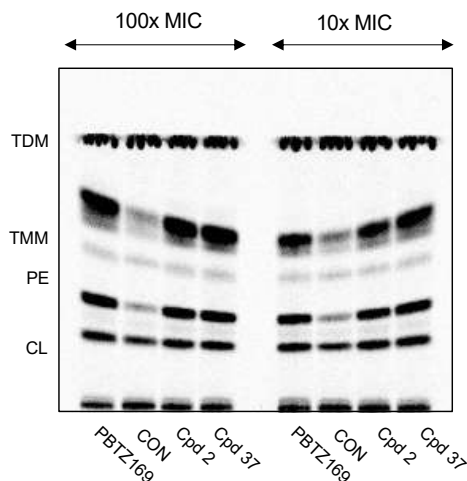
Figure 3. TLC analysis of the [^{14}C]-acetate labelled lipids, extracted from Mtb H37Rv. Control: TDM, trehalose dimycolates; TMM, trehalose monomycolates; PE, phosphatidylethanolamine; CL, cardiolipin.

3.5. Metabolic Stability, Cytotoxicity and Solubility of Selected Compounds

Since compounds **2**, **31**, **34**, **37** and **40** showed higher inhibition potentials against DrpE1, their metabolic stability in human microsomes was then examined (**Table 4**). As expected, the metabolic stability was affected by the linker portion. Among them, compound **2** containing an 1,2,3-triazole linker had the highest stability (T$_{1/2}$=100.4 min) and the lowest intrinsic clearance Cl$_{int}$ (17.31 mL/min/kg), followed by compound **36** with an 1,2,4-oxadiazole linker (T$_{1/2}$=68.2 min, and Cl$_{int}$=25.48 mL/min/kg). The thiazole linker compound **34** was the least stable.

Table 4. Metabolic stability of compounds **2**, **31**, **34**, **37** and **40** in human microsomes.

	2	**31**	**34**	**37**	**40**
$T_{1/2}$ (min)	100.4	33.6	24.3	68.2	34.3
Cl_{int}(mL/min/kg)	17.31	51.71	71.60	25.48	50.68

Compounds **2** and **37** were further examined for cytotoxicity against HepG2 cell using an MTT assay[15]. No inhibition of cell viability was observed at concentration lower than 1.0 µg/mL (supporting information, Figure S1). At 5.0 µg/mL, cell viability was reduced to 72–75%.

The compound solubility is closely related to its bioavailability and *in vivo* activity, thus the kinetic solubility of compounds **2** and **37** was determined. In PBS buffer, both compounds exhibited higher solubility than PBTZ169 (supporting information,Table S2), which also correlated with their reduced clogP values.

3.6. Pharmacokinetics and Efficacy of Compounds 2 and 37

To further characterize compounds **2** and **37**, we evaluated their pharmacokinetic profiles in mice. BALB/C mice were given compounds **2** or **37** intravenously (i.v., 2 mg/kg) or orally (p.o., 10 mg/kg). As shown in **Table 5**, both compounds had acceptable PK profiles with good oral bioavailability of 35.7% and 70.6%, respectively. The $T_{1/2}$ and C_{max} values were shorter than PBTZ169[16], which was dosed orally at 25 mg/kg.

Table 5. Pharmacokinetic parameters for compounds **2** and **37**.

PK parameters	Compound **2**		Compound **37**	
	PO	IV	PO	IV
C_{max}(ng·mL^{-1})	1798.5	1250.0	1891.3	1860.8
$t_{1/2}$ (h)	1.3	1.1	0.6	0.3
MRT (h)	2.0	1.5	0.9	0.4
AUC (h·ng/mL)	2185.6	1210.6	1865.2	528.1
Cl_{int} (mL/h/kg)		1670.2		3837.4
F (%)	35.7		70.6	

C_{max}, maximum concentration of drug in blood plasma; $t_{1/2}$, the elimination half-life of drug; MRT, mean residence time; AUC, area under the curve; Cl_{int}, hepatic clearance; F, oral bioavailability. Dose: i.v., 2 mg/kg; p.o., 10 mg/kg.

The anti-TB potential of the compounds was evaluated using a mouse model acutely infected with *Mtb* H37Rv. Both compounds were administered, oral dose 50 mg/kg for 4 weeks, once per day except weekends. PBTZ169 killed Mtb by 3 logs in the lungs compared to the control group (**Figure 4**). By comparison, compound **37** reduced the bacteria load by 1.2 logs, compound **2** barely displayed efficacy.
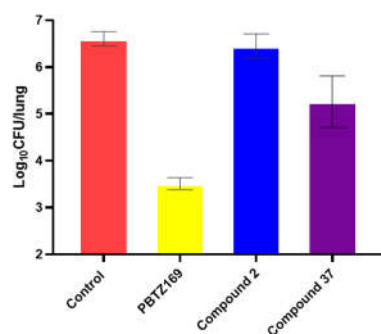
Figure 4. Efficacy of compound **2** and **37** in BALB/C mice (*n* = 6) infected with *M. tuberculosis* H37Rv.

4. Discussion

BTZ derivatives have been reported to exhibit potent antimycobacterial activity *in vitro* and *in vivo*, the two analogs BTZ043 and PBTZ169 are being evaluated in clinical trials[17,18]. However, the poor solubility and high plasma binding for both compounds indicate their physiochemical properties are far from optimal[19], thus improvement of the BTZ compounds drug-like properties has been a continuous effort in the research community[19,20].

We previously reported a series of BTZ derivatives with 6-methansulfonyl replacement of 6-CF$_3$, along with side chain modification. The optimized BTZ analogs displayed more than 20–fold increased aqueous solubility than that of PBTZ169[11]. With MIC values in 10–40 nM ranges and acceptable pharmacokinetic properties, we recently performed the compound efficacy study in the TB infected mice model. Unfortunately, no obvious CFU reduction (data not reported) was recorded. Nonetheless, our side chain modification strategy highlights alternatives to focus on the linker and tail position, a concerted modification might provide candidates with improved physiochemical properties and high *in vivo* efficacy.

Herein, we investigated analogs with the original 6-CF$_3$ BTZ pharmacophore in combination with our modified side chain moieties. These novel series of compounds exhibited MICs values 5–7 folds lower than that of the corresponding 6-methansulfonyl counterparts, indicating the original 6-CF$_3$ BTZ core structure is more favorable. By performing the DprE1 enzyme activity assay and the cell wall synthesis disruption experiments, we demonstrated the compounds on target inhibitory activity, in accordance with that of PBTZ169. The optimized compound in this novel series of BTZ analogs displayed good PK profile in the mice TB model.

This study demonstrated that our side chain modification approach provided a BTZ derivative with efficacy of reducing the bacteria load in lung 1.2 logs. Factors to influence the compound *in vivo* efficacy are complex, we noticed that the PK parameter $t_{1/2}$ for PBTZ 169 was longer than compound **37**[16], that may partially explain the observed potency difference. Our study also shown that the compounds metabolic stability was closely related to the linker moiety, the $t_{1/2}$ for the triazole linker compound was 5-folds longer than the thiozole linker, suggesting further linker exploration might provide more metabolically stable compounds. Finally, the presence of a basic nitrogen in the side chain of PBTZ169 greatly increased the compound solubility in acidic condition, which facilitated the compound's gastric absorption[21]. While the lack of such a basic center in neutral compound **37** might be unbeneficical, further investigation by introducing a basic or polar atom at appropriate position might be worthy of being explored.

5. Conclusions

In the present work, a new series of BTZ derivatives were prepared. We linked the BTZ core structure with aryl groups using different heterocycles as linkers: including 1,3,4-triazole, oxazole, thiazole, 1,2,4-oxadiazole and 1,2,4-thiadiazole. Compared to the previously reported compounds, these novel BTZ derivatives displayed increased mycobacteria inhibitory activity and metabolic stability. The represented compounds exhibited single digit nanomolar MICs values, low cytotoxicity against mammalian cell. One compound displayed *in vivo* efficacy, although much worse than the

PBTZ169 compound. The study highlighted our side chain modification strategy and expanded the diversity of BTZ compounds. Further linker and side chain modification to increase the compound *in vivo* potency is going on and will be reported in due course.

Supplementary Materials: The synthetic procedure of reaction intermediates, DprE1 enzyme IC$_{50}$s aqueous solubility and cytotoxicity information were provided in the supporting information, which can be downloaded at the website of this paper posted on Preprints.org, Figure S1: Inhibitory activity of compounds 2 and 37 against HepG2 cell; Table S1: MIC (H37Rv) and DprE1 inhibitory IC$_{50}$ for selected compounds and Table S2: Kinetic solubility of compounds 2 and 37 in 50 mM PBS at pH 7.2

Author Contributions: D.F. and B.W. contributed equally. C. Q. conceived the idea and wrote the manuscript. D.F., R.S., and X. W. synthesized the compounds. B. W. and Y. L. designed and performed the compounds MIC determination. G.S. and L.R.C designed and determined the compounds inhibitory activity against DprE1. K.S. and K.M. designed and performed the metabolic labeling experiment. O.R. and V.M. designed and performed the *in vivo* efficacy experiments. Y.H. analyzed the data and wrote the manuscript. All authors have given approval to the final version of the manuscript.

Funding: Funded by The Priority Academic Program Development of the Jiangsu Higher Education Institutes (PAPD); Italian Ministry of Education, University and Research (MIUR) (Dipartimenti di Eccellenza, Program 2018-2022) to Department of Biology and Biotechnology, University of Pavia (L.R.C.); the Ministry of Education, Science, Research and Sport of the Slovak Republic (grant VEGA 1/0301/18); the Operation Program of Integrated Infrastructure for the project, Advancing University Capacity and Competence in Research, Development and Innovation, ITMS2014+: 313021X329, co-financed by the European Regional Development Fund. National Natural Science Foundation of China (32170032), National Major Youth Talent Project A, Jiangsu Specially-appointed Professor Project, Suzhou Innovation Leading Talent Project (ZXL2022456), and a Start Fund of Soochow University.

Institutional Review Board Statement: Not applicable.

Informed Consent Statement: Not applicable.

Data Availability Statement: Not applicable.

Conflicts of Interest: The authors declare no conflict of interest.

References

1. *Global Tuberculosis Report 2022*; **2022**, World Health Organization
2. Gauri S. Shetye, Scott G. Franzblau, and Sanghyun Cho, New tuberculosis drug targets, their inhibitors, and potential therapeutic impact, *Transl. Res.*, **2020**, *220*, 68–97.
3. Makarov, V.; Manina, G.; Mikušová, K.; Mollmann, U.; Ryabova, O.; Saint-Joanis, B.; Dhar, N.; Pasca, M. R.; Buroni, S.; Lucarelli, A. P.; Milano, A.; De Rossi, E.; Beláňová, M.; Bobovská, A.; Dianišková, P.; Korduláková, J.; Sala, C.; Fullam, E.; Schneider, P.; McKinney, J. D.; Brodin, P.; Christophe, T.; Waddell, S.; Butcher, P.; Albrethsen, J.; Rosenkrands, I.; Brosch, R.; Nandi, V.; Bharath, S.; Gaonkar, S.; Shandil, R. K.; Balasubramanian, V.; Balganesh, T.; Tyagi, S.; Grosset, J.; Riccardi, G.; and Cole, S. T. Benzothiazinones kill *Mycobacterium tuberculosis* by blocking arabinan synthesis, *Science*, **2009**, *324*, 801–804.
4. Trefzer, C.; Škovierová, H.; Buroni, S.; Bobovská, A.; Nenci, S.; Molteni, E.; Pojer, F.; Pasca, M. R.; Makarov, V.; Cole, S. T.; Riccardi, G.; Mikušová, K.; and Johnsson, K., Benzothiazinones are suicide inhibitors of mycobacterial decaprenylphosphoryl-beta-D-ribofuranose 2'-oxidase DprE1. *J. Am. Chem. Soc*. **2012**, *134*, 912–915.
5. Neres, J.; F. Pojer, E. M.; Chiarelli, L. R.; Dhar, N.; Boy-Rottger, S.; Buroni, S.; Fullam, E.; Degiacomi, G.; Lucarelli, A. P.; Read, R. J.; Zanoni, G.; Edmondson, D. E.; De Rossi, E.; Pasca, M.; McKinney, R. J. D.; Dyson, P. J.; Riccardi, G.; Mattevi, A.; Cole, S. T.; Binda, C. Structural basis for benzothiazinone-mediated killing of *Mycobacterium tuberculosis*. *Sci. Transl. Med*. **2012**, *4*, 150ra121.
6. Makarov, V.; Lechartier, B.; Zhang, M.; Neres, J.; van der Sar, A. M.; Raadsen, S. A.; Hartkoorn, R. C.; Ryabova, O. B.; Vocat, A.; Decosterd, L. A.; Widmer, N.; Buclin, T.; Bitter, W.; Andries, K.; Pojer, F.; Dyson, P. J.; Cole. S. T. Towards a new combination therapy for tuberculosis with next generation benzothiazinones, *EMBO Mol. Med.*, **2014**, *6*, 372–383.
7. Zhang, G.; Howe, M.; and Aldrich, C. C.; Spirocyclic and bicyclic 8-nitrobenzothiazinones for Tuberculosis with improved physicochemical and pharmacokinetic properties, *ACS Med. Chem. Lett*. **2019**, *10*, 348−351.
8. Rui S.; Bin W.; Giovanni S.; Xiaomei W.; Yuanyuan S.; Yue W.; Xin W.; Laurent R. C.; Yu L.; and Chunhua Q. Development of 6-methanesulfonyl-8-nitrobenzothiazinone based antitubercular agents, *ACS Med. Chem. Lett*. **2022**, *13*, 593−598.

9. Liu, L.; Kong, C.; Fumagalli, M.; Savkova, K.; Xu, Y.; Huszar, S.; Sammartino, J. C.; Fan, D.; Chiarelli, L. R.; Mikusova, K.; Sun, Z.; Qiao, C. Design, synthesis and evaluation of covalent inhibitors of DprE1 as antitubercular agents. *Eur. J. Med. Chem.*, **2020**, *208*, 112773.

10. Neres, J.; Hartkoorn, R. C.; Chiarelli, L. R.; Gadupudi, R.; Pasca, M. R.; Mori, G.; Venturelli, A.; Savina, S.; Makarov, V.; Kolly, G. S.; Molteni, E.; Binda, C.; Dhar, N.; Ferrari, S.; Brodin, P.; Delorme, V.; Landry, V.; de Jesus Lopes Ribeiro, A. L.; Farina, D.; Saxena, P.; Pojer, F.; Carta, A.; Luciani, R.; Porta, A.; Zanoni, G.; De Rossi, E.; Costi, M. P.; Riccardi, G.; Cole, S. T. 2-Carboxyquinoxalines kill Mycobacterium tuberculosis through noncovalent inhibition of DprE1. *ACS Chem. Biol.* **2015**, *10*, 705–714.

11. Dongguang F.; Bin W.; Stelitano, G.; Savková, K., Shi, R. Huszár, S., Han, Q., Mikusová, K., Chiarelli, L. R., Lu, Y., Chunhua, Q.; Structure and activity relationships of 6-sulfonyl-8-nitrobenzothiazinones as antitubercular agents, *J. Med. Chem.* **2021**, *64*, 14526−14539.

12. Kumari, S.; Carmona, A. V.; Tiwari, A. K.; Trippier, P. C. Amide bond bioisosteres: strategies, synthesis, and successes, *J. Med. Chem.* **2020**, *63*, 12290−12358.

13. Gillis, E. P.; Eastman, K. J.; Hill, M. D.; Donnelly, D. J.; Meanwell, N. A. Applications of fluorine in medicinal chemistry, *J. Med. Chem.* **2015**, *58*, 8315–8359.

14. Karabanovich, G., Dusek, J.; Savkova,K.; Pavlis,O.; Pavkova,I.; Korabecny, J.; Kucera,T.; Vlckova, H. K.; Huszar, S.; Konyarikova, Z.; Konecna, K.; Jandourek,O.; Stolarikova, J.; Kordulakova, J.; Vavrova, K.; Pavek, P.; Klimesova,V.; Hrabalek, A.; Mikusova K.; Roh J.   Development of 3,5-dinitrophenyl-containing 1,2,4-triazoles and their trifluoromethyl analogues as highly efficient antitubercular agents inhibiting decaprenylphosphoryl-β-D-ribofuranose 2'-oxidase. *J. Med. Chem.*, **2019**, *62*, 8115–8139.

15. Yang, J.; Liu, Y.; Xue, C.; Yu, W.; Zhang, J.; Qiao, C. Synthesis and biological evaluation of glaucocalyxin A derivatives as potential anticancer agents, *Eur. J. Med. Chem.* **2014**, *86*, 235–241.

16. Makarov. V.; Cole. S. T. 2-Piperazine-1-yl-4*H*-1,3-benzothiazin-4-one derivatives and their use for the treatment of mammalian infections, WO 2012/066518A1.

17. https://www.newtbdrugs.org/pipeline/compound/btz-043.

18. https://www.newtbdrugs.org/pipeline/compound/macozinone-mcz-pbtz-169.

19. Tiwari, R.; Mollmann, U.; Cho, S.; Franzblau, S. G.; Miller, P. A.; Miller, M. J. Design and syntheses of anti-Tuberculosis agents inspired by BTZ043 using a scaffold simplification strategy, *ACS Med. Chem. Lett.*, **2014**, *5*, 587−591.

20. Piton, J.; Vocat, A.; Lupien, A.; Foo, C. S.; Riabova, O.; Makarov, V.; Cole. S. T., Structure-based drug design and characterization of sulfonyl piperazine benzothiazinone inhibitors of DprE1 from Mycobacterium tuberculosis, *Antimicrob. Agents & Chemother.*, **2018**, *62*, e00681–18.

21. Makarov V.; Mikušová, K., Development of Macozinone for TB treatment: an update. *Appl. Sci.* **2020**, *10*, 2269;